
HOW GOOD NEURAL NETWORKS INTERPRETATION METHODS REALLY ARE? A QUANTITATIVE BENCHMARK.

Antoine Passemiers^{1,*}, Pietro Folco^{2,*}, Daniele Raimondi^{1,†}, Giovanni Birolo², Yves Moreau¹, Piero Fariselli²

ABSTRACT

Saliency Maps (SMs) have been extensively used to interpret deep learning models decision by highlighting the features deemed relevant by the model. They are used on highly nonlinear problems, where linear feature selection (FS) methods fail at highlighting relevant explanatory variables. However, the reliability of gradient-based feature attribution methods such as SM has mostly been only qualitatively (visually) assessed, and quantitative benchmarks are currently missing, partially due to the lack of a definite ground truth on image data. Concerned about the apophenic biases introduced by visual assessment of these methods, in this paper we propose a synthetic quantitative benchmark for Neural Networks (NNs) interpretation methods. For this purpose, we built synthetic datasets with nonlinearly separable classes and increasing number of *decoy* (random) features, illustrating the challenge of FS in high-dimensional settings. We also compare these methods to conventional approaches such as mRMR or Random Forests. Our results show that our simple synthetic datasets are sufficient to challenge most of the benchmarked methods. TreeShap, mRMR and LassoNet are the best performing FS methods. We also show that, when quantifying the relevance of a few non linearly-entangled predictive features diluted in a large number of irrelevant noisy variables, neural network-based FS and interpretation methods are still far from being reliable.

1 Introduction

Decision processes are different in machines and humans. The training of Neural Networks (NNs) is solely guided by the minimizing of a loss function, which incidentally and only partially aligns with human understanding of the problem, since the optimization of the loss function relies on the labeling of training samples rather than articulate expert insights, eventually making these models diverge from human expectations. An extreme example of such divergence are *Clever Hans* predictors, which exclusively rely on dataset artifacts [1]. More often, their decision processes are influenced by contextual features which are not necessary causal, and which are thus acting as confounders (e.g. presence of wooden hurdles in horse pictures). Therefore, *Clever Hans* predictors can appear proficient on training data but remain prone to potentially high generalization error in unseen settings or on independent test data (e.g. absence of wooden hurdles in horse pictures).

For these reasons, interpretability has become an emerging crucial aspect of Machine Learning (ML), and solutions for Explainable Artificial Intelligence (XAI) [1] are now also ethical requirements posed by institutions like the European Union [2]. In many *real-life* applications, a clear understanding of the model decision-making process is indeed necessary for its adoption in a production environment. Interpretability is even more relevant in the context of nonlinear techniques with strong prediction power and modeling capabilities such as Deep Neural Networks (DNN) [1], since linear models are notoriously easier to explain and can therefore be complemented with simple but sound and effective FS methods (LASSO [3], shrunken centroid method [4]) that exploits the additivity of input variables [5].

Due to the intrinsic human-readability properties of simpler models (i.e. linear models, decision trees), they are often preferred in critical settings. On the other hand, complex nonlinear models such as DNNs exploit non-trivial

¹ESAT-STADIUS, KU Leuven, Leuven, Belgium

²Department of Medical Sciences, University of Torino, Torino, Italy

*These authors contributed equally to this work.

[†]Corresponding author: daniele.raimondi@kuleuven.be

interactions between input features, making them a model-of-choice for solving difficult tasks that require higher abstraction (e.g. Genome interpretation, protein folding and human-level real-time control [6, 7, 8, 9]). In theory, DNNs can ignore irrelevant features during the training phase, but this depends on the optimizer and the loss function landscape, which can be highly non-convex.

In recent years, gradient-based *a posteriori* interpretation methods for DNNs such as Saliency Maps (SMs) rapidly gained popularity [10]. The most common approaches include Integrated Gradients [11], DeepLift [12], Input \times Gradient [13], SmoothGrad [14] and Guided Backpropagation [15]. They can be easily applied to any NN model with libraries such as Captum [16].

These methods have been developed mainly in the context of computer vision, and their ability to identify the *salient* pixels for the classification of images was primarily qualitatively assessed by visually inspecting the obtained SMs in relation to the input images, because there was no *ground truth* for what should be considered salient, since this concept is intrinsically model-dependent. To the best of our knowledge, quantitative benchmarks of the reliability of SM interpretations is currently missing, especially on non-image data. At the same time, several studies showing puzzling SM interpretation results and perplexing behaviors have been already published, raising concerns about these methods [17, 18, 19].

The interpretation of non-linear model is an extremely active field of research and, besides *a posteriori* interpretation methods such as SMs, in recent years several DNNs architectures incorporating FS capabilities have been developed, such as CancelOut [20], DeepPINK [21], LassoNet [22], FSNet [23], Concrete Autoencoder [24] and Diet-Net [25].

In this paper, we benchmarked the most recent nonlinear FS and interpretation methods for DNNs on synthetic, simplistic, yet challenging artificial datasets, comparing them with older and more conventional FS approaches. Each of our datasets consists of few (2-7) variables that jointly and nonlinearly correlate with the output class, as well as a variable number of irrelevant random features (decoys). To allow fair assessment, both relevant and irrelevant variables have been sampled with the exact same variance: each feature follows a uniform marginal distribution in 4 out of 5 of our datasets. In our fifth dataset, features have been simply standardized. In this way, methods that exploit variance signatures, such as Principal Component Analysis are not applicable. These datasets have been constructed in such a way that the classes cannot be segregated by linear decision boundaries, making linear FS methods totally unsuitable for the problem at hand. The synthetic nature of the datasets grants us complete knowledge of the predictive signal and allows us to quantitatively benchmark the ability of nonlinear FS methods to detect nonlinearly and jointly relevant features in controlled sample-to-feature ratio experimental settings. As baseline methods, we used additional FS methods that are not based on NNs, like Random forests (RFs) or minimum redundancy maximum relevance (mRMR).

Our results show that the DNN-based FS methods tested are not able to extract relevant features if they are diluted in a random set of noisy variables. Conversely, feature relevances extracted from RFs are more reliable on average. We obtained similar results while benchmarking several SM a posteriori interpretation methods. These results indicate that the field of FS and DNNs interpretation needs to further refine the available methods, and suggest that a standardized *quantitative validation* of the newly proposed methods should be used to assess their performance and limits, to give users a more realistic idea of the situations in which these approaches are actually reliable.

2 Methods

2.1 Benchmark datasets

2.1.1 Uniformly-distributed variables

We first built four datasets representing archetypal nonlinear binary classification tasks. Each dataset contains $n = 1000$ observations and $m = p + k$ features, uniformly distributed in the $[0, 1]$ interval. p and k denote the number of predictive and irrelevant features, respectively. Each dataset was then built by attributing a label to data points according to a nonlinear combination of the predictive features. All the remaining features are effectively random with respect to the labels, and thus act as decoys when it comes to feature selection. The number of positives is equal to the number of negatives, to prevent any artifact due to class imbalance. Here we describe the different characteristics of each outcome (label). They are also visually shown in Fig. 1.

- RING: positive labels are associated to the points that form a bi-dimensional ring, defined by the features in positions $j \in \{0, 1\}$. The total number of predictive features is 2. Points where assigned to the positive class when:

$$|\sqrt{(x_0 - 0.5)^2 + (x_1 - 0.5)^2} - 0.35| \leq 0.1151$$

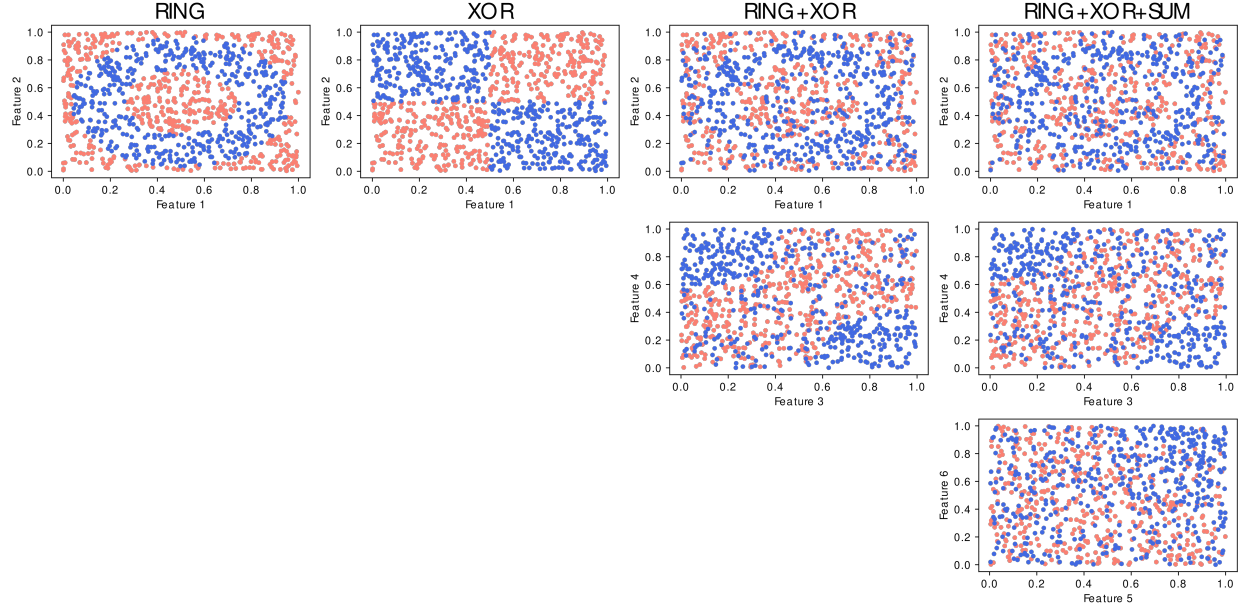


Figure 1: The four datasets, with their predictive features shown by pairs. Orange and blue correspond to the positive and negative classes, respectively. Each column is associated with one dataset, and each row corresponds to a distinct features pair.

- XOR: the bi-dimensional space formed by the features in position $j \in \{0, 1\}$ is divided into 4 identical regions. Points in the upper left and lower right quadrants are labelled as positive samples. The total number of predictive features is 2. Points were considered positive when:

$$(x_0 - 0.5)(0.5 - x_1) \geq 0$$

- RING+XOR: the samples that are either positive samples in the RING dataset (considering the features in position $j \in \{0, 1\}$) or positive samples in the XOR dataset (considering the features in positions $j \in \{2, 3\}$) are positive. This dataset thus contains 4 predictive features, in positions $j \in \{0, 1, 2, 3\}$. Points were considered positives when they satisfied any of the following:

$$\begin{aligned} |\sqrt{(x_0 - 0.5)^2 + (x_1 - 0.5)^2} - 0.35| &\leq 0.0704 \\ (x_2 - 0.5)(0.5 - x_3) &\geq 0.0337 \end{aligned}$$

- RING+XOR+SUM: the samples that are positive in the RING, XOR datasets or such that $x_4 + x_5 + \epsilon > 0.5$ are positive samples. x_j denotes the j -th feature and ϵ is Gaussian noise sampled from $\mathcal{N}(\mu = 0, \sigma = 0.2)$. Like in the RING and XOR datasets, the corresponding predictive features $\{0, 1, 2, 3\}$ do not contain noise. In RING+XOR+SUM the predictive features are in positions $\{0, 1, 2, 3, 4, 5\}$. See Suppl. Fig. 4 for a visual explanation. Points were considered positives when they satisfied at least one of the following inequalities:

$$\begin{aligned} |\sqrt{(x_0 - 0.5)^2 + (x_1 - 0.5)^2} - 0.35| &\leq 0.0479 \\ (x_2 - 0.5)(0.5 - x_3) &\geq 0.0598 \\ x_4 + x_5 + \mathcal{N}(\mu = 0, \sigma = 0.2) &\geq 1.4074 \end{aligned}$$

The four outcomes are shown in Fig.1.

2.1.2 Gaussian graphical model

While for sufficiently large values of m the datasets defined above are already challenging, we built an additional dataset (called DAG) characterized also by confounding effects. Indeed, these effects occur in most real-life settings, and are very likely to *misguide* the different models towards learning predictive patterns from irrelevant associations. This dataset has been generated by a directed Gaussian graphical model. The exact procedure is detailed in Suppl. Mat. 1.1. By construction, features can be categorized based on their degree of relevance:

- Features X_i that are highly relevant as they are causal for the target variable Y : $X_i \rightarrow \dots \rightarrow Y$
- Features X_i that are weakly relevant as they correlate with the target variable only due to indirect effects, like in forks: $X_i \leftarrow \dots \leftarrow X_j \rightarrow \dots \rightarrow Y$
- Irrelevant features

2.2 Benchmark procedure

We assessed the reliability of FS methods on nonlinear ML tasks with a growing degree of difficulty by incrementally diluting the relevant features in the uniformly-distributed datasets. An exponential increase of the number k of decoy features is added in each run: $m \in \{2, 4\} \cup K$ for XOR and RING datasets, $m \in \{4\} \cup K$ for RING+XOR and $m \in \{6\} \cup K$ for RING+XOR+SUM, where $K = \{8, 16, 32, 64, 128, 256, 512, 1024, 2048\}$. For each run, we set the number of samples to $n = 1000$.

For each run and dataset, we assessed the performance of both predictors and FS methods. First, for each embedded FS method that relies on a predictive model, we evaluated the latter using a 6-fold cross-validation procedure. Then we computed the AUROC and AUPRC of each step accordingly. We also reported these metrics for a baseline NN without prior or posterior FS. In the paper, we simply refer to it as “Neural Network”.

Second, we evaluated the ability of each FS algorithm to rank the predictive features higher than the decoys. More specifically, we quantified the latter as the percentage of predictive features among the highest p and $2p$ top-ranked features, where p corresponds to the number of truly predictive features in each dataset ($p = 2$ for XOR and RING, $p = 4$ for RING+XOR, $p = 6$ for RING+XOR+SUM, $p = 7$ or 81 in DAG depending on the definition used). We refer to them as best p and best $2p$ scores for short. To ensure fair comparison, and avoid assigning good performance to badly-designed FS methods (where feature importances are influenced by their position/indices in the data matrix), we randomly permuted the columns of the input data matrix in each fold of the k -fold cross-validation procedure. For feature attribution methods (e.g. saliency maps), only the points from the held-out sets of the 6-fold cross-validation have been used to select features.

2.3 Machine Learning models

To ensure a fair comparison between NN-based FS methods, we tried to reuse the same neural architecture whenever possible. By default, NNs have been implemented with Pytorch [26]. The data has been centered by replacing each input vector x_i by $2x_i - 1$, so each feature ranges between -1 and 1 . The default model is a three-layer perceptron with LeakyReLU activation functions, with a 0.2 slope for negative values. The 2 hidden layers have 16 neurons each. Additionally, L2 regularisation on the parameters is used, with a regularisation parameter of 10^{-2} . The model was trained with the Adam optimizer [27] for up to 1000 epochs, with a learning rate of 0.005 and a batch size of 64. A scheduler guided the optimisation of each model by adjusting the learning rate over time, decreasing it by a 0.9 factor every time the total loss function stagnates for 10 epochs (with a cooldown of 5 epochs). Gaussian noise, with a standard deviation of 0.05, was added to the inputs in order to regularise the models further. In order to minimize overfitting risks and get the best out of each NN-based approach, we implemented an early stopping criterion. We saved the NN parameters at each epoch and kept the ones that minimize the loss function on a held-out set composed of 20% of the training data. The training was interrupted prematurely if the validation loss had not decreased during the last 5 epochs.

All feature attribution methods are based on the architecture described above. However, due to the peculiarities of some embedded FS methods or the constraints of their implementation, these latter methods might build on subtle variants of this architecture. When relevant, these differences are explained in the next section.

2.4 Feature selection methods

The benchmarked algorithms belong to three categories: feature attribution, embedded, and filter methods. We now describe them in details.

2.4.1 Feature attribution methods

Feature attribution methods propose an *a posteriori* interpretation of the method M by approximately reconstructing the decision process followed by M in order to produce the prediction y_i . Gradient-based interpretation methods for NNs like Saliency Maps (SMs) belong to this category. Given a trained NN model M , the forward pass $M(x_i)$ of sample x_i is computed, alongside with the gradient $\partial M(x_i)/\partial x_i$ of the target output $y_i = M(x_i)$ with respect to the input x_i . The gradient values identify which positions in x_i are the most relevant for the prediction. Indeed,

because the gradient points towards the direction of steepest descent, the highest components of the gradient indicate which input variables require the least change to produce the largest variation in the output y_i . In this study we used the Captum [16] library to benchmark the Integrated Gradients [11], Saliency [10], DeepLift [12], Input \times Gradient [13], SmoothGrad [14], Guided Backpropagation [15]. From the same library, we also benchmarked non-gradient-based interpretation methods like Deconvolution [28], Feature Ablation, Feature Permutation [29] and Shapley Value [30] interpretation approaches. For SmoothGrad, data was injected with random noise sampled from a zero-centered Gaussian distribution with 0.1 standard deviation (Captum’s implementation of NoiseTunnel). The operation has been repeated 50 times per input vector. For the Integrated Gradients, DeepLift, Feature Ablation and Shapley Value Sampling methods, the 0 vector was supplied as baseline point. The baseline point is used for different purposes depending on the method. For example, the basepoint provided for the Integrated Gradients method defines the point from which to compute the integral and smooth the feature attribution vector. Because all these gradient-based methods only provide instance-level feature importances, we computed the overall feature importances as the average of absolute values of the instance-level importances. Because it was *a priori* unclear to us whether these instance-level scores should be computed on the training set or the validation set (with their difference explained by the generalization error), we compared the two settings in section 3.7.

2.4.2 Embedded FS methods

The second category of FS approaches are the embedded methods, which operate *at training time*, such as FSNet [23], Concrete Autoencoder [24], CancelOut [20], Random Forest [31], DeepPINK [21] and LassoNet [22]. In particular, FSNet and Concrete Autoencoder jointly *rank* features and train the model.

FSNet’s architecture is composed of a selector and an encoder network, which branches into a classifier and a final sub-network comprising a decoder and a reconstruction layer. The selector consists in a matrix multiplication operation, involving a low-rank matrix of shape $k \times 2p$ obtained from a weights predictor, followed by a softmax activation (after addition of Gumbel noise to the logits): $2p$ features are selected, and we computed both best p and best $2p$ scores using the feature importances as proposed in [23]. The weights predictor of the selector is composed of a fully-connected layer with no activation. We chose the identity function as activation for both the encoder and decoder, as no further refinement of the input features was deemed necessary. The reconstruction layer is the reverse operation of the selector network, and performs a matrix multiplication analogously. The corresponding low-rank matrix is predicted from a predictor module composed of a fully-connected layer with no activation. The classifier has the same architecture as described in the previous section, except that its input size is restricted to $2p$. The whole model was trained for 2000 epochs. 30 bins (latent size of 10) were used to compute the inputs frequencies necessary to predict the low-rank matrices.

CancelOut is composed of the common architecture described in the previous section (trained in the same manner), preceded by a CancelOut layer. We experimented with 2 variants of the method: 1) with a Sigmoid activation and CancelOut weights regularisation (we denote the corresponding model by CancelOut Sigmoid for short), and 2) with a Softmax activation layer and without regularization (CancelOut Softmax). In the former case, we used a $\lambda_1 = 0.2$ coefficient for the variance and a $\lambda_2 = 0.1$ for the regularisation term. Because L1 regularisation encourages importances weights to converge to 0.5 (sigmoid(0) = 0.5), we replaced it by the sum of CancelOut weights, unlike the original implementation. Indeed, this choice of regularisation better promotes sparsity among feature importances. In both cases, CancelOut weights were initialised with the same value $\beta = 1$. The model has been trained for 300 epochs, as the convergence of CancelOut weights requires longer time than the optimisation of the classifier alone.

All models built for evaluating the LassoNet [22] feature selection method contained 32 hidden neurons and ReLU activation functions, as only the latter were available among activation functions in the `lassonet` Python package.

To evaluate the Concrete Autoencoder (CAE), we used the `concrete-autoencoder` Python package [24], and implemented the underlying classifier with Keras [32] in accordance with the architecture described in the previous section. The CAE has been trained for 300 epochs, with initial temperature 10 and final temperature 0.01. The CAE has been trained twice, once for selecting p and once for selecting $2p$ features. The model has been trained for 10 epochs. Each hidden layer is composed of 32 neurons, and followed by a 20% dropout.

DeepPINK requires knockoff features, that we generated in two different ways depending on the nature of the dataset. For the DAG dataset, we relied on the framework of Model-X Knockoff features designed by Candès et al. [33]. Details of Model-X Knockoff features are explained in Suppl. Mat. 1.2. For the remaining 4 datasets, knockoff features were generated by simply sampling a uniform distribution (the marginal distribution of the original data matrix X is multivariate but uniform).

Random forests were grown with the Scikit-learn Python package [34] and are composed of 500 trees each. We used the default parameters. We selected features from trained random forests using the widely-used impurity-based feature importance scores, as implemented in Scikit-Learn. More specifically, the importance of a feature is defined as the total reduction in Gini impurity caused by all node splits involving that feature, averaged across all trees in the forest.

2.4.3 Filter methods

The last category of methods that we considered is the filter-method algorithms, such as Relief [35] or minimum redundancy maximum relevance (mRMR) [36]. These methods do not assign predictions; therefore no AUROC or AUPRC values are reported. mRMR relies on statistical measures such as mutual information [37], which requires a discretisation of the input variables. Therefore, we divided each feature into 20 equally-sized bins, which we are sufficiently thin for capturing the nonlinear dependencies, and sufficiently large for robust estimation (~ 40 observations per bin). AUROC and AUPRC were computed for FS methods based on a predictive model, and reported as a function of the input feature size.

3 Results

Feature Selection (FS) is widely used across many fields of science [38, 39, 40]. The goal of FS algorithms is to identify or rank features in function of the *predictive signal* they carry with respect to a prediction label. In this study we benchmarked 20 FS methods on 5 synthetic datasets (RING, XOR, RING+XOR, RING+XOR+SUM and DAG) providing nonlinear binary classification tasks (see Methods). These datasets represent classical ML problem, such as the XOR problem, the discrimination of points lying on a ring-shaped subspace and combinations thereof (see Methods for more details).

3.1 Random forests outperform other methods on RING by a large margin

In the RING dataset, positive labels are associated to the points lying on a bi-dimensional ring defined by features in positions 0, 1 (see Suppl. Fig. S1).

Top panels in Fig. 2 show the AUROC and AUPRC of all trained models, as a function of the total number of features $m = p + k$. It is noteworthy that all models but the Random Forest have AUROCs and AUPRCs approaching a random predictor (50%) for values of m greater than 32. This effect is consistent with the percentages of relevant features reported in the bottom graphs of panel Fig. 2. Both Random forests and TreeSHAP perfectly re-identified the relevant features, even when $m = 2048$. However, their decaying performance (as m increases) suggest that tree-based models may lose their FS capabilities in extremely high-dimensional ($m \gg 2048$).

3.2 Neural networks are better suited for solving the XOR problem

As shown in Fig. 3, NN models obtained overall better results, and mRMR underperformed, even for a small number of irrelevant features k . In particular, LassoNet reached maximal best p and best $2p$ scores for each m , and $> 90\%$ AUROC and AUPRC for each $m \leq 512$. This relatively high predictive performance of LassoNet can be attributed to the internal cross-validation procedure used to find the optimal degree of sparsity of the NN parameters. The FS methods, besides LassoNet, that found the highest proportions of relevant features are Relief, CancelOut Sigmoid, and feature attribution methods like DeepLift or Deconvolution. Most methods undergo drastic performance losses when $m \geq 128$.

3.3 RF, mRMR and LassoNet are the best performing methods on RING+XOR

This dataset comprises four relevant features ($p = 4$). Similarly to what we observed for the RING dataset, we see from Fig. 4 and Tab. 2 that Random Forests and TreeSHAP (which interprets learned Random Forests) perform the best, along with mRMR. Random Forests achieve high AUROC and AUPRC values and correctly rank the features in most settings. In particular, it constitutes the only FS method capable of ranking over the 60% of relevant features among the top 4 features for $m \leq 2048$. For any other method to achieve a similar percentage of relevant features selected $> 80\%$, the total number of features needs to be decreased to $m = 16$, thus requiring to make the problem orders of magnitude simpler. Among these remaining methods, mRMR dominates regardless of the number of features. Overall, only RF, mRMR and LassoNet result in best p and best $2p$ scores $> 50\%$ when $m > 256$. All remaining methods except LassoNet appear to perform close to random for $m \geq 256$. LassoNet starts performing random for $m \geq 1024$.

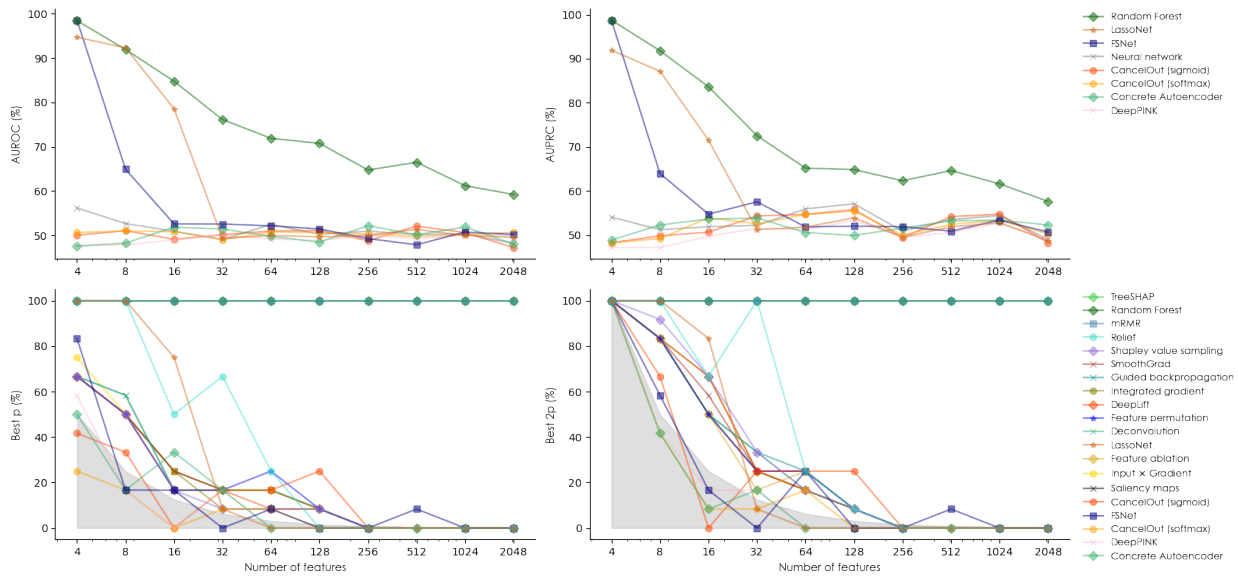


Figure 2: Performance of the different models and feature selection methods on the RING dataset. (Top) AUROC and AUPRC of each trained model as a function of the number of features. (Bottom) Percentage of relevant features selected by each FS method in the top p and $2p$, respectively. Shaded areas correspond to the best p and best $2p$ scores of a dummy FS method that performs worse than random. Methods have been sorted by decreasing order of average performance in the legend.

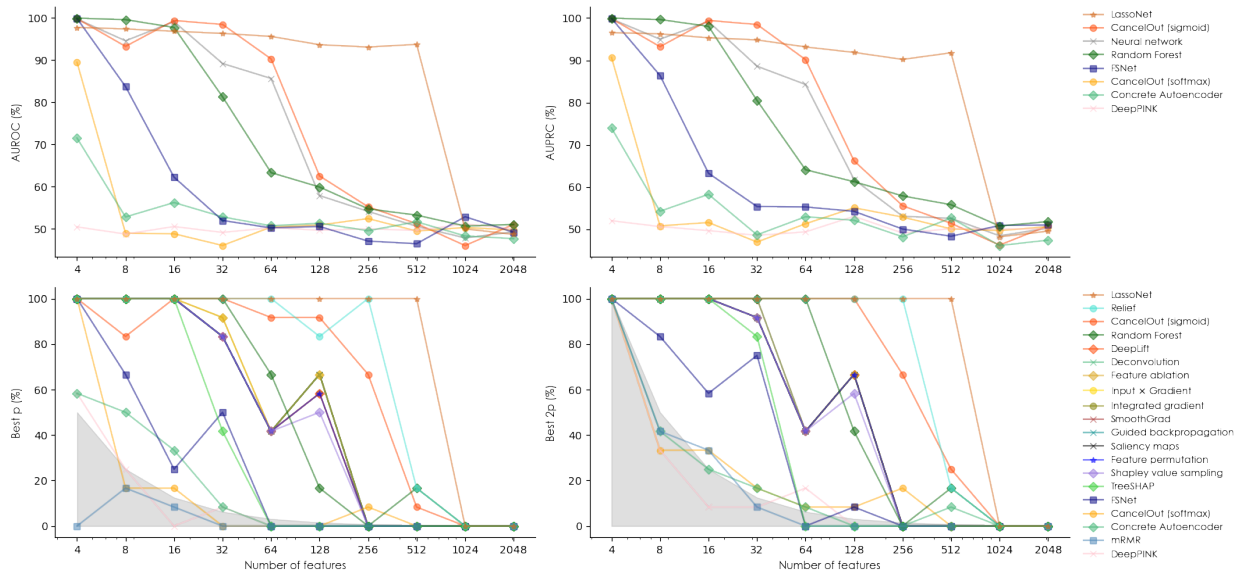


Figure 3: Performance of the different models and feature selection methods on the XOR dataset. (Top) AUROC and AUPRC of each trained model as a function of the number of features. (Bottom) Percentage of relevant features selected by each FS method in the top p and $2p$, respectively. Shaded areas correspond to the best p and best $2p$ scores of a dummy FS method that performs worse than random. Methods have been sorted by decreasing order of average performance in the legend.

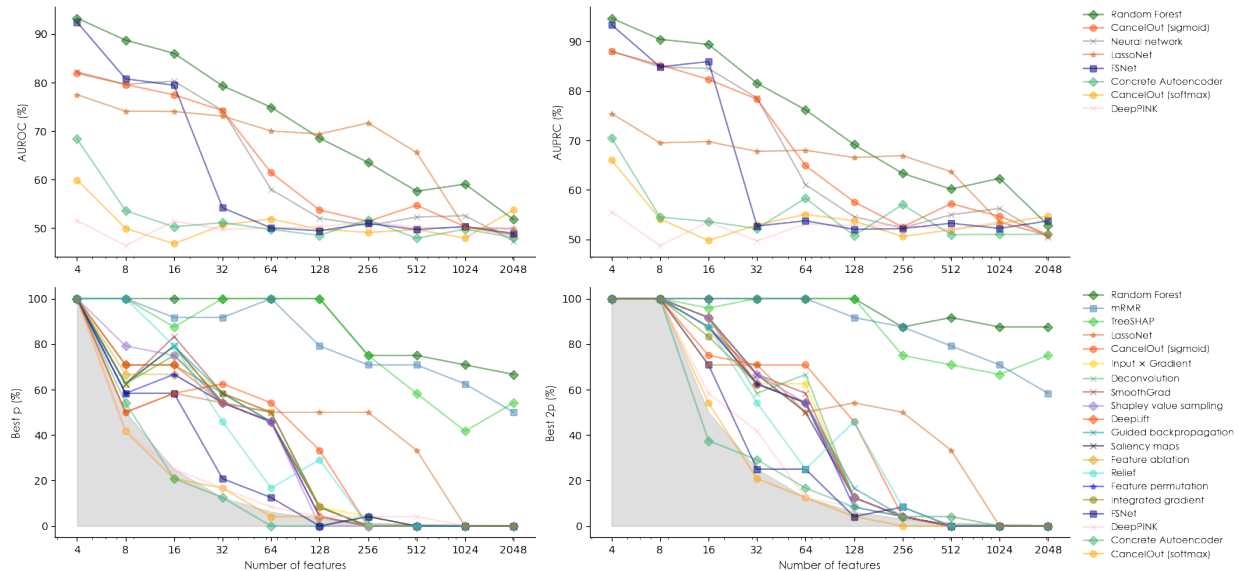


Figure 4: Performance of the different models and feature selection methods on the RING+XOR dataset. (Top) AUROC and AUPRC of each trained model as a function of the number of features. (Bottom) Percentage of relevant features selected by each FS method in the top p and $2p$, respectively. Shaded areas correspond to the best p and best $2p$ scores of a dummy FS method that performs worse than random. Methods have been sorted by decreasing order of average performance in the legend.

3.4 RING+XOR+SUM is challenging for all methods

There are six relevant features in this dataset, two of them being linear with some additive noise. The prediction problem appears to be quite difficult, with AUROC and AUPRC values < 0.85 even for $p = 6$ when no decoy feature is added (see Fig. 5). Contrary to the previous experiments, overall performance drops gradually with m . This can be explained by the slightly larger number of relevant features ($p = 6$) as well as their heterogeneity, allowing models to detect the features that are the easiest to pick, given the characteristics of each model (XOR features for NNs, RING features for mRMR and tree-based models, SUM features for most models). RF/TreeSHAP and mRMR are the best FS methods, with the best p scores $\geq 40\%$ and the best $2p$ scores $\geq 60\%$ for each value of m . Concrete autoencoder ranks last as FS method, and DeepPINK ranks last as a predictive model. Finally, we observe that CancelOut Sigmoid clearly outperforms its softmax variant by a large margin.

3.5 Disentangling causal from spurious effects on DAG is too challenging for FS methods

In the fifth and last dataset in this benchmark, which has been generated by a graphical model (see Methods), relevant features can be defined either as features that are causal for the observed variable Y , or features that are expected to correlate with Y due to indirect (confounding) effects. We refer to this dataset as DAG. In Table 1, we reported the best p and $2p$ scores based on these two definitions. We can see that, in both settings, TreeSHAP and its underlying Random Forest model are outperforming other methods. Concrete autoencoder, FSNet, CancelOut (softmax) and DeepPINK fail at detecting relevant features. Among feature attribution methods, Input \times Gradient, Feature permutation and Shapley value sampling slightly improve over the other methods. Overall, none of the benchmarked approaches seems to be relatively better at disentangling indirect correlations from causal effects on the DAG dataset.

3.6 Benchmark summary

Complementary to the presented figures, we summarised in Tab. 2 the best p and best $2p$ scores for all FS methods on each dataset. For readability purposes, we only report the mean scores, computed across all values of m . The table is organised in two parts: instance-level feature attribution methods (*a posteriori* gradient-based methods such as Saliency Maps), and the remaining approaches. Best performing methods from each category are highlighted in bold. Among model-based and *a priori* FS techniques, TreeSHAP and its underlying model Random Forests both

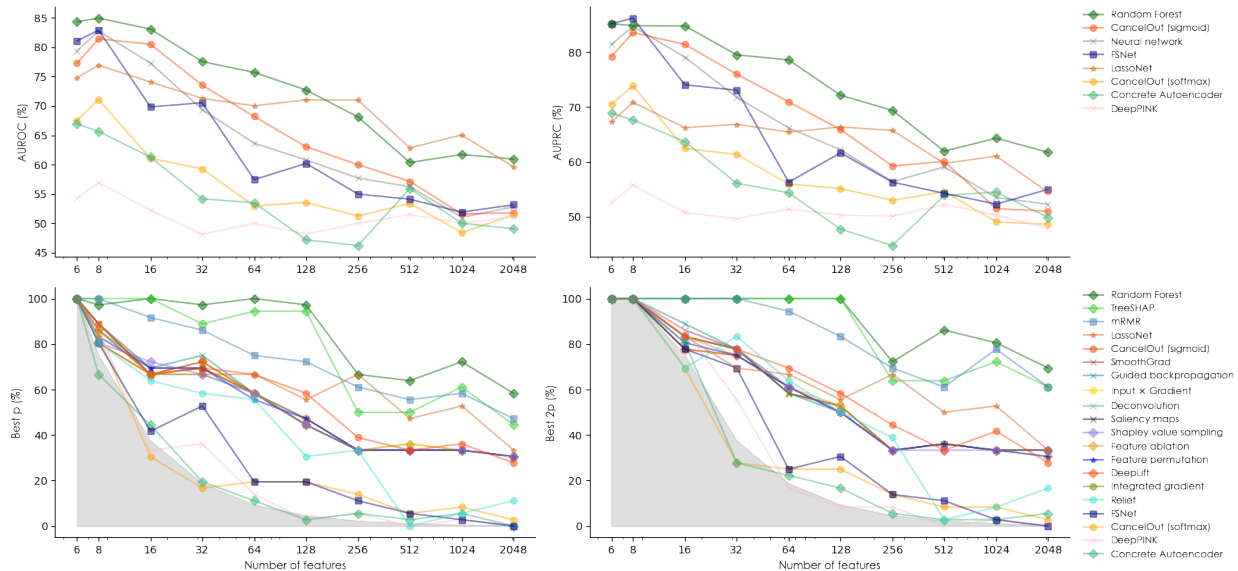


Figure 5: Performance of the different models and feature selection methods on the RING+XOR+SUM dataset. (Top) AUROC and AUPRC of each trained model as a function of the number of features. (Bottom) Percentage of relevant features selected by each FS method in the top p and $2p$, respectively. Shaded areas correspond to the best p and best $2p$ scores of a dummy FS method that performs worse than random. Methods have been sorted by decreasing order of average performance in the legend.

outperform all approaches by a large margin on all datasets but XOR. Overall, mRMR appears to be the second best-performing technique, despite its underperformance on XOR. Complementary to mRMR, LassoNet achieved maximal performance on XOR, while getting average results on the remaining datasets.

Instance-level *a posteriori* methods do not show significant differences, except on the DAG dataset. In the latter setting, Input \times Gradient, Feature Ablation and Shapley value sampling seem to perform relatively better.

In order to compare the methods in situations where the curse of dimensionality is exacerbated, we reported the same results on sub-sampled versions of the same datasets, with $n \in \{250, 500\}$. These results are shown in Supp. Tables 1 and 2. We observed that mRMR, tree-based methods and LassoNet consistently outperform other methods in the same settings.

3.7 Bootstrapping influences the quality of feature attribution scores

Since practitioners may use *a posteriori* SM methods in different ways, and since it was unclear whether using points from the training set can indeed improve the quality of feature ranking, we investigated whether the latter can benefit from bootstrapping and the use of the training set. In the first setting, we computed one feature importance vector per instance from the held-out set after training, and averaged them across the whole held-out set. In a second stage, we added a bootstrapping component by repeating this step 10 times and re-training the model each time on a random sample composed of 80% of the training set (sampling with replacement). The final importance vectors have been obtained by averaging across the 10 runs. In the third setting, we removed bootstrapping but computed the feature importance vectors on the points from the training set only, and left the held-out set unused.

4 Discussion

4.1 Feature selection and modeling quality are interdependent

Care should be taken in interpreting the results presented in our study. Indeed, each FS method necessarily relies on some modeling assumptions, and the relevance of selected features is heavily impacted by the model’s adequacy to the data. In particular, the inference process does not guarantee to yield the optimal solution (the set of parameters that produces the least generalisation error). Despite the flexibility of NNs, as described by the universal approximation

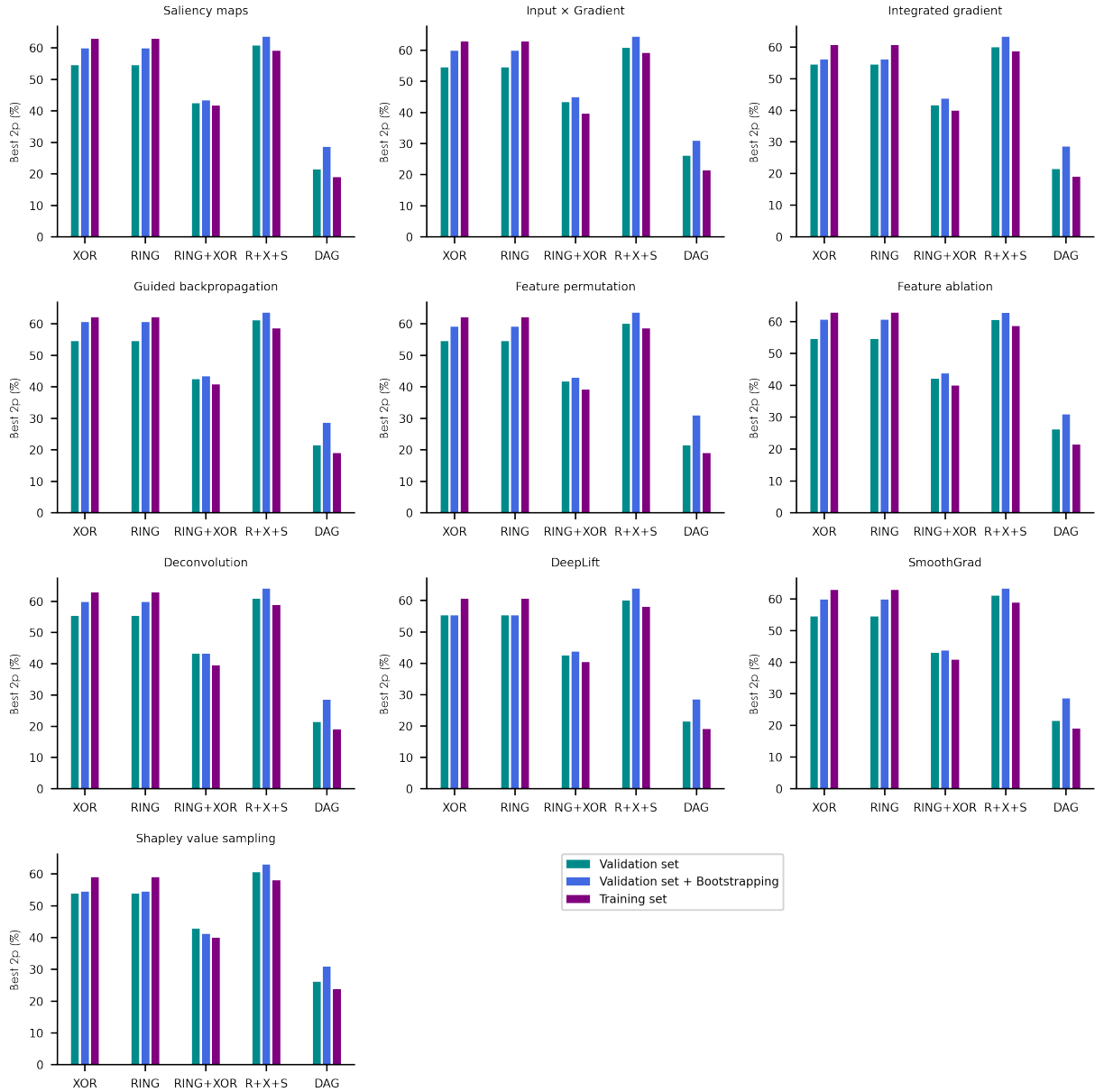


Figure 6: Average best $2p$ score on each of the 5 datasets, using three different approaches to infer feature importances from instance-level feature attribution methods. In the first setting, only the points from the held-out set have been used to rank features. In the second case, bootstrapping was performed by randomly sampling (with replacement) 80% of the training set before training the NN. In the last setting, only the points from the training set have been used.

Dataset	% causal features		% correlated features		Performance (%)	
	Best p	Best 2p	Best p	Best 2p	AUROC	AUPRC
Saliency maps	14.3	21.4	9.5	14.6	-	-
Integrated gradient	14.3	21.4	9.7	14.6	-	-
DeepLift	14.3	21.4	9.7	14.6	-	-
Input \times Gradient	19.0	26.2	10.1	14.2	-	-
SmoothGrad	14.3	21.4	9.5	14.6	-	-
Guided backpropagation	14.3	21.4	9.5	14.6	-	-
Deconvolution	14.3	21.4	9.5	14.6	-	-
Feature ablation	19.0	26.2	9.7	14.2	-	-
Feature permutation	16.7	21.4	10.3	14.4	-	-
Shapley value sampling	16.7	26.2	10.3	14.6	-	-
mRMR	16.7	19.0	6.6	11.5	-	-
LassoNet	14.3	14.3	6.8	11.1	71.9	66.0
Relief	14.3	14.3	6.8	9.5	-	-
Concrete Autoencoder	2.4	11.9	4.9	8.0	50.1	52.8
FSNet	2.4	4.8	3.5	7.2	56.7	55.5
CancelOut (softmax)	2.4	4.8	5.8	8.2	46.5	48.5
CancelOut (sigmoid)	16.7	21.4	9.7	13.8	56.2	56.8
DeepPINK	0.0	0.0	4.3	8.4	50.0	50.0
Random Forest	21.4	40.5	12.8	17.9	75.4	73.9
TreeSHAP	28.6	42.9	13.4	17.3	-	-

Table 1: Best p and best 2p scores of all feature selection methods on the DAG dataset. $p = 7$ when considering only causal features as relevant (first multi-column) and $p = 81$ when also including confounders (second multi-column). Additionally, AUROC and AUPRC scores have been reported for embedded methods.

theorem [41] for example, the optimal architecture choice (with smallest generalisation error) is unknown and can only be found by cross-validation. The eventual lack of regularisation, coupled with the presence of a large number of input features, therefore increasing the effective number of parameters, is likely to drive the model towards learning from irrelevant correlations. In such case, because the model’s decision process relies on irrelevant features, the FS method building on this model will necessarily attach higher importance to those features. Therefore, FS techniques based on NNs might be hard to exploit in practice, as they require building the most accurate model, and guiding the inference process to the optimal solution. This goal is easier to reach when provided with sufficiently deep insights about the data. In this sense, FS resembles a chicken-and-egg problem, and because of that FS methods cannot be blindly applied on a dataset without minimal prior knowledge of the data and the limitations of the model used.

In particular, all feature attribution / SM methods considered in this study, as well as many of the other FS techniques, rely on a neural network that requires proper training. Because the number of parameters varied with the number of input features, it remains highly probable that the corresponding models either under- or overfitted the data in some situations, regardless of the presence of dropout and L2 regularisation. Overall, there is no guarantee that the Adam optimizer consistently guided the model to the globally-optimal solution, or that the generalisation error was minimal.

4.2 Tree-based modeling and decision tree induction are two separate concepts

Random forests have largely outperformed other methods on the RING, RING+XOR, RING+XOR+SUM and DAG datasets, both as a FS technique and as predictive models. However, the dataset where RFs perform comparatively (to other methods) worse is XOR, which consists of data points obeying a simple logical rule. Such rule can be perfectly captured through a piece-wise linear function. In particular, among all off-the-shelf ML models, decision trees are the optimal choice for modeling such data, as only three decision splits should be theoretically sufficient for perfect segregation of the classes. However, performance of RFs is sub-optimal as observed in Fig. 3.

Dataset Method	RING		XOR		RING+XOR		RING+XOR+SUM		DAG	
	Best k	Best 2k	Best k	Best 2k	Best k	Best 2k	Best k	Best 2k	Best k	Best 2k
Saliency maps	25.8	34.8	53.8	54.5	35.0	42.5	56.1	60.8	14.3	21.4
Integrated gradient	24.2	36.4	53.0	54.5	35.4	41.7	55.3	60.0	14.3	21.4
DeepLift	24.2	36.4	53.0	55.3	34.6	42.5	55.3	60.0	14.3	21.4
Input \times Gradient	26.5	34.8	54.5	54.5	35.8	43.3	55.8	60.8	19.0	26.2
SmoothGrad	25.8	36.4	53.8	54.5	36.2	42.9	56.1	61.1	14.3	21.4
Guided backpropagation	25.8	36.4	53.8	54.5	35.4	42.5	56.4	61.1	14.3	21.4
Deconvolution	25.8	35.6	53.8	55.3	35.0	43.3	55.6	60.8	14.3	21.4
Feature ablation	25.0	34.8	54.5	54.5	34.2	42.1	56.1	60.6	19.0	26.2
Feature permutation	25.8	35.6	53.0	54.5	32.9	41.7	55.6	60.0	16.7	21.4
Shapley value sampling	23.5	37.9	52.3	53.8	35.4	42.9	55.3	60.6	16.7	26.2
mRMR	100.0	100.0	12.5	28.3	81.7	88.8	74.7	84.7	16.7	19.0
LassoNet	34.8	35.6	81.8	81.8	44.6	52.9	64.2	67.8	14.3	14.3
Relief	40.2	45.5	72.7	74.2	37.1	42.1	43.9	53.3	14.3	14.3
Concrete Autoencoder	19.7	24.2	22.7	27.3	19.2	30.0	25.8	36.4	2.4	11.9
FSNet	21.2	28.0	31.1	38.6	25.4	33.3	33.3	43.1	2.4	4.8
CancelOut (softmax)	14.4	25.0	22.0	28.8	18.8	29.2	30.0	38.1	2.4	4.8
CancelOut (sigmoid)	21.2	31.1	67.4	72.0	35.8	46.7	58.6	63.6	16.7	21.4
DeepPINK	17.4	25.0	17.4	24.2	20.4	32.9	28.1	37.8	0.0	0.0
Random Forest	100.0	100.0	54.5	59.8	88.8	95.4	85.3	90.8	21.4	40.5
TreeSHAP	100.0	100.0	40.2	43.9	81.7	88.3	78.3	86.1	28.6	42.9

Table 2: Best k and best 2k score percentages on the 5 datasets. For the first 4 datasets, scores have been averaged over $m \in \{2, 4, 6, 8, 16, 32, 64, 128, 256, 512, 1024, 2048\}$. Top and bottom parts of the table correspond to instance-level feature attribution and embedded/filter FS methods, respectively. Best performing methods are highlighted in bold.

The quality of its feature selection and prediction is not linked to the sophistication of the modeling *per se*, but rather the optimality of the decision tree induction algorithm. Indeed, Scikit-learn’s implementation is based on the heuristic CART algorithm [42], which is unlikely to infer the tree with highest information gain and minimal number of nodes. In particular in the XOR dataset, selecting one of the two relevant features as first decision split is not sufficient, as it does not produce any change in the class proportions within the newly obtained hyper-parallelipipeds. Therefore, RFs are counter-intuitively better at growing from ring-shaped data, since any split on one of the 2 corresponding features results in an increase of class purity (strictly positive information gain). On the XOR dataset, optimal inference would require a lookahead of 1 feature, or bivariate decision splits. In conclusion, the relatively lower performance of RFs on the XOR dataset can mostly be attributed to the sub-optimality of its underlying tree induction algorithm.

4.3 Univariate feature selection remains relevant in a high dimensionality context

Although the datasets have been constructed in a way that they are highly challenging for both linear and univariate FS methods, it must be noted that (nonlinear) univariate filter methods remain highly relevant in some contexts. First, they are computationally more efficient (and embarrassingly parallel), making them competitive in a high-dimensional setting (e.g. Whole Genome Sequencing data). Second, they are still capable of capturing relevant features when they *individually* correlate with the explained variable, in a nonlinear fashion. This is shown by the maximal performance (100% best p score for any value of m) of mutual information (MI) on the RING dataset (as shown in Suppl. Tab. 3), suggesting that mutual information (MI) consistently detects the reduction of entropy caused by the ring-shaped function that generated the data. Indeed, this ring-shaped data is leaking information about the class at the level of individual features (the probability distribution of each feature is altered, when conditioned on the class distribution). Because real-life problems are more likely to exhibit univariate nonlinear correlations than our artificial datasets, simple information-theoretic approaches could remain highly relevant. However, data availability is a crucial prerequisite for accurate estimation of MI.

5 Conclusion

In this paper, we investigated the usefulness of nonlinear FS approaches in the case of high-dimensional data with a low sample-to-feature ratio. What emerges from the results is that Random Forests and Relief outperform neural network-based approaches on all datasets that exhibit nonlinear correlations between individual features and the target

variable (all but the XOR dataset). Therefore, DNN models might not be the best choice for feature selection on datasets with these characteristics, i.e. a low density of relevant features, a prevalence of nonlinear patterns and variance homogeneity (for both predictive and decoy features). In real-life applications, we mainly encounter that relationships among the features in the data tend to be additive. However, our study indicates that when both additive and nonlinearly entangled features are present, we can only see the former unless a considerable number of samples are available compared to the input feature size.

References

- [1] Sebastian Lapuschkin, Stephan Wäldchen, Alexander Binder, Grégoire Montavon, Wojciech Samek, and Klaus-Robert Müller. Unmasking clever hans predictors and assessing what machines really learn. *Nature communications*, 10(1):1–8, 2019.
- [2] Andreas Holzinger, Peter Kieseberg, Edgar Weippl, and A Min Tjoa. Current advances, trends and challenges of machine learning and knowledge extraction: from machine learning to explainable ai. In *International Cross-Domain Conference for Machine Learning and Knowledge Extraction*, pages 1–8. Springer, 2018.
- [3] Seung-Jean Kim, Kwangmoo Koh, Michael Lustig, Stephen Boyd, and Dimitry Gorinevsky. An interior-point method for large-scale ℓ_1 -regularized least squares. *IEEE journal of selected topics in signal processing*, 1(4):606–617, 2007.
- [4] Robert Tibshirani, Trevor Hastie, Balasubramanian Narasimhan, and Gilbert Chu. Diagnosis of multiple cancer types by shrunken centroids of gene expression. *Proceedings of the National Academy of Sciences*, 99(10):6567–6572, 2002.
- [5] Trevor Hastie, Robert Tibshirani, and Jerome Friedman. *The elements of statistical learning: data mining, inference and prediction*. Springer, 2 edition, 2009.
- [6] Daniele Raimondi, Massimiliano Corso, Piero Fariselli, and Yves Moreau. From genotype to phenotype in arabidopsis thaliana: in-silico genome interpretation predicts 288 phenotypes from sequencing data. *Nucleic acids research*, 50(3):e16–e16, 2022.
- [7] John Jumper, Richard Evans, Alexander Pritzel, Tim Green, Michael Figurnov, Olaf Ronneberger, Kathryn Tunyasuvunakool, Russ Bates, Augustin Žídek, Anna Potapenko, et al. Highly accurate protein structure prediction with alphafold. *Nature*, 596(7873):583–589, 2021.
- [8] Volodymyr Mnih, Koray Kavukcuoglu, David Silver, Andrei A Rusu, Joel Veness, Marc G Bellemare, Alex Graves, Martin Riedmiller, Andreas K Fidjeland, Georg Ostrovski, et al. Human-level control through deep reinforcement learning. *nature*, 518(7540):529–533, 2015.
- [9] Alex Graves, Greg Wayne, Malcolm Reynolds, Tim Harley, Ivo Danihelka, Agnieszka Grabska-Barwińska, Sergio Gómez Colmenarejo, Edward Grefenstette, Tiago Ramalho, John Agapiou, et al. Hybrid computing using a neural network with dynamic external memory. *Nature*, 538(7626):471–476, 2016.
- [10] Karen Simonyan, Andrea Vedaldi, and Andrew Zisserman. Deep inside convolutional networks: Visualising image classification models and saliency maps. *arXiv preprint arXiv:1312.6034*, 2013.
- [11] Mukund Sundararajan, Ankur Taly, and Qiqi Yan. Axiomatic attribution for deep networks. *CoRR*, abs/1703.01365, 2017.
- [12] Avanti Shrikumar, Peyton Greenside, and Anshul Kundaje. Learning important features through propagating activation differences. *CoRR*, abs/1704.02685, 2017.
- [13] Avanti Shrikumar, Peyton Greenside, Anna Shcherbina, and Anshul Kundaje. Not just a black box: Learning important features through propagating activation differences. *CoRR*, abs/1605.01713, 2016.
- [14] Daniel Smilkov, Nikhil Thorat, Been Kim, Fernanda B. Viégas, and Martin Wattenberg. Smoothgrad: removing noise by adding noise. *CoRR*, abs/1706.03825, 2017.
- [15] Jost Tobias Springenberg, Alexey Dosovitskiy, Thomas Brox, and Martin Riedmiller. Striving for simplicity: The all convolutional net. *arXiv preprint arXiv:1412.6806*, 2014.
- [16] Narine Kokhlikyan, Vivek Miglani, Miguel Martin, Edward Wang, Jonathan Reynolds, Alexander Melnikov, Natalia Lunova, and Orion Reblitz-Richardson. Pytorch captum. <https://github.com/pytorch/captum>, 2019.
- [17] Julius Adebayo, Justin Gilmer, Michael Muelly, Ian Goodfellow, Moritz Hardt, and Been Kim. Sanity checks for saliency maps. *Advances in neural information processing systems*, 31, 2018.

- [18] Ahmed Alqaraawi, Martin Schuessler, Philipp Weiß, Enrico Costanza, and Nadia Berthouze. Evaluating saliency map explanations for convolutional neural networks: a user study. In *Proceedings of the 25th International Conference on Intelligent User Interfaces*, pages 275–285, 2020.
- [19] Weili Nie, Yang Zhang, and Ankit Patel. A theoretical explanation for perplexing behaviors of backpropagation-based visualizations. In *International Conference on Machine Learning*, pages 3809–3818. PMLR, 2018.
- [20] Vadim Borisov, Johannes Haug, and Gjergji Kasneci. Cancelout: A layer for feature selection in deep neural networks. In *International Conference on Artificial Neural Networks*, pages 72–83. Springer, 2019.
- [21] Yang Young Lu, Yingying Fan, Jinchu Lv, and William Stafford Noble. Deeppink: reproducible feature selection in deep neural networks. *arXiv preprint arXiv:1809.01185*, 2018.
- [22] Ismael Lemhadri, Feng Ruan, Louis Abraham, and Robert Tibshirani. Lassonet: A neural network with feature sparsity. *Journal of Machine Learning Research*, 22(127):1–29, 2021.
- [23] Dinesh Singh, Héctor Climente-González, Mathis Petrovich, Eiryō Kawakami, and Makoto Yamada. Fsnnet: Feature selection network on high-dimensional biological data. *arXiv preprint arXiv:2001.08322*, 2020.
- [24] Abubakar Abid, Muhammad Fatih Balin, and James Zou. Concrete autoencoders for differentiable feature selection and reconstruction. *arXiv preprint arXiv:1901.09346*, 2019.
- [25] Adriana Romero, Pierre Luc Carrier, Akram Erraqabi, Tristan Sylvain, Alex Auvolat, Etienne Dejoie, Marc-André Legault, Marie-Pierre Dube, Julie G. Hussin, and Yoshua Bengio. Diet networks: Thin parameters for fat genomics. In *International Conference on Learning Representations*, 2017.
- [26] Adam Paszke, Sam Gross, Francisco Massa, Adam Lerer, James Bradbury, Gregory Chanan, Trevor Killeen, Zeming Lin, Natalia Gimelshein, Luca Antiga, Alban Desmaison, Andreas Kopf, Edward Yang, Zachary DeVito, Martin Raison, Alykhan Tejani, Sasank Chilamkurthy, Benoit Steiner, Lu Fang, Junjie Bai, and Soumith Chintala. Pytorch: An imperative style, high-performance deep learning library. In *Advances in Neural Information Processing Systems 32*, pages 8024–8035. Curran Associates, Inc., 2019.
- [27] Diederik P Kingma and Jimmy Ba. Adam: A method for stochastic optimization. *arXiv preprint arXiv:1412.6980*, 2014.
- [28] Aravindh Mahendran and Andrea Vedaldi. Salient deconvolutional networks. In *European Conference on Computer Vision*, pages 120–135. Springer, 2016.
- [29] Christoph Molnar. *Interpretable machine learning*. Lulu. com, 2020.
- [30] Javier Castro, Daniel Gómez, and Juan Tejada. Polynomial calculation of the shapley value based on sampling. *Computers & Operations Research*, 36(5):1726–1730, 2009.
- [31] Leo Breiman. Random forests. *Machine learning*, 45(1):5–32, 2001.
- [32] Francois Chollet et al. Keras, 2015.
- [33] Emmanuel Candès, Yingying Fan, Lucas Janson, and Jinchu Lv. Panning for gold: ‘model-x’ knockoffs for high dimensional controlled variable selection. *Journal of the Royal Statistical Society: Series B (Statistical Methodology)*, 80(3).
- [34] F. Pedregosa, G. Varoquaux, A. Gramfort, V. Michel, B. Thirion, O. Grisel, M. Blondel, P. Prettenhofer, R. Weiss, V. Dubourg, J. Vanderplas, A. Passos, D. Cournapeau, M. Brucher, M. Perrot, and E. Duchesnay. Scikit-learn: Machine learning in Python. *Journal of Machine Learning Research*, 12:2825–2830, 2011.
- [35] S Francisca Rosario and K Thangadurai. Relief: feature selection approach. *International journal of innovative research and development*, 4(11), 2015.
- [36] Hanchuan Peng, Fuhui Long, and Chris Ding. Feature selection based on mutual information criteria of max-dependency, max-relevance, and min-redundancy. *IEEE Transactions on pattern analysis and machine intelligence*, 27(8):1226–1238, 2005.
- [37] Alexander Kraskov, Harald Stögbauer, and Peter Grassberger. Estimating mutual information. *Physical review E*, 69(6):066138, 2004.
- [38] Giovanna Nicora, Francesca Vitali, Arianna Dagliati, Nophar Geifman, and Riccardo Bellazzi. Integrated multi-omics analyses in oncology: a review of machine learning methods and tools. *Frontiers in oncology*, 10:1030, 2020.
- [39] Parminder S Reel, Smarti Reel, Ewan Pearson, Emanuele Trucco, and Emily Jefferson. Using machine learning approaches for multi-omics data analysis: A review. *Biotechnology Advances*, 49:107739, 2021.

- [40] Daniele Raimondi, Gabriele Orlando, Wim F Vranken, and Yves Moreau. Exploring the limitations of biophysical propensity scales coupled with machine learning for protein sequence analysis. *Scientific reports*, 9(1):1–11, 2019.
- [41] George Cybenko. Approximation by superpositions of a sigmoidal function. *Mathematics of control, signals and systems*, 2(4):303–314, 1989.
- [42] Leo Breiman, Jerome H Friedman, Richard A Olshen, and Charles J Stone. *Classification and regression trees*. Routledge, 2017.